ARTICLE NO. 77-1133

# Observations on Maximum Likelihood Estimation of Aerodynamic Characteristics from Flight Data

Kenneth W. Iliff* and Richard E. Maine†
*NASA Dryden Flight Research Center, Edwards, Calif.*

**This paper discusses the application of a maximum likelihood estimation method to flight test data. The results are based on 11 years' experience of estimating stability and control derivatives from 3000 maneuvers from 30 aircraft. Flight results are presented from recent studies on understanding the discrepancies previously observed in the magnitude of the Cramer-Rao bounds, on the scale effects on the derivative estimates obtained from dynamic aircraft flight maneuvers, and on the analysis of lateral-directional maneuvers obtained in turbulence.**

## Nomenclature

$a_y$ = lateral acceleration, $g$
$C_{l_\beta}$ = coefficient of roll due to sideslip, per deg
$C_{n_r}$ = coefficient of yaw due to yaw rate, per rad
$C_{n_\beta}$ = coefficient of yaw due to sideslip, per deg
$C_{n_{\delta_r}}$ = coefficient of yaw due to rudder deflection, per deg
$f(\cdot)$ = general function
$g(\cdot)$ = general function
$G$ = spectral density of measurement noise
$J$ = cost functional
$n$ = state noise vector
$p$ = roll rate, deg/s
$\hat{p}_g$ = gust roll rate, deg/s
$\bar{q}$ = dynamic pressure, N/m$^2$
$r$ = yaw rate, deg/s
$R$ = covariance of weighted residual measurement error
$t$ = time, s
$\Delta t$ = sample interval, s
$T$ = total time, s
$u$ = control vector
$x$ = state vector
$y$ = observation vector
$y_\xi$ = computed observation vector based on $\xi$
$z$ = measured observation vector
$\hat{z}_\xi$ = Kalman-filtered estimate of the observation vector
$\alpha$ = angle of attack, deg
$\beta$ = angle of sideslip, deg
$\hat{\beta}_g$ = gust angle of sideslip, deg
$\delta_a$ = aileron deflection, deg
$\eta$ = measurement noise vector
$\xi$ = vector of unknown parameters
$\varphi$ = bank angle, deg
$\omega$ = frequency, rad/s
$\omega_0$ = true frequency, rad/s

*Superscript*

$*$ = matrix transpose

Presented as Paper 77-1133 at the AIAA 4th Atmospheric Flight Mechanics Conference, Hollywood, Fla., Aug. 8-10, 1977; submitted Sept. 23, 1977; revision received June 30, 1978. 

Index categories: Aerodynamics; Testing, Flight and Ground; Handling Qualities, Stability and Control.

*Aerospace Engineer. Associate Fellow AIAA.
†Aerospace Engineer. Member AIAA.

## Introduction

MAXIMUM likelihood estimation[1] has become the primary technique for estimating the stability and control derivatives from flight test data. The authors' organization has been using this estimation technique since 1966. Much of the experience gained has been reported in Refs. 2 and 3, but many questions and applications remain to be investigated. The authors' organization has continued to investigate the application of maximum likelihood estimation methods to the analysis of a wide variety of aircraft flight test situations. This paper presents a review of some of these recent studies; additional results are presented in Ref. 4.

## Maximum Likelihood Estimation

The maximum likelihood estimation method[1,5] is one technique that can be used to estimate unknown coefficients of a dynamic system. The mathematical model of this dynamic system may, in most instances, be described as

$$\dot{x}(t) = f(x,u,n,t)$$

$$y(t) = g(x,u,t)$$

$$z(t) = y(t) + \eta(t)$$

The state and measurement noise vectors are assumed to be Gaussian white. The maximum likelihood estimates are obtained by maximizing the log likelihood functional, the form of which depends on the type of the dynamic equations. This is actually done by minimizing the negative of the log likelihood functional. If there is no state noise, the cost functional to be minimized is

$$J = \frac{1}{T}\int_0^T [z(t)-y_\xi(t)]^*(GG^*)^{-1}[z(t)-y_\xi(t)]\,dt \qquad (1)$$

where $G$ is the spectral density of the measurement noise. A more complete discussion of this cost functional is given in Ref. 6.

If the system to be analyzed is described by a linear set of dynamic equations that include state noise, the cost functional to be minimized is

$$J = \frac{1}{T}\int_0^T [z-\hat{z}_\xi]^*(GG^*)^{-1}[z-\hat{z}_\xi]\,dt + \text{trace}\,(R) \qquad (2)$$

where $\hat{z}_\xi$ is the Kalman-filtered[7] estimate of $y$, and $R$ is the covariance matrix of the weighted observation estimation

error. This algorithm,[7-10] in contrast to the extended Kalman filter method,[11] uses the Kalman filter to estimate only the states and measurements and not to estimate the unknown coefficients. Equation (2) is equivalent to Eq. (1) if there is no state noise, because $\hat{z}_\xi$ is then equivalent to $y_\xi$ and $R$ is the null matrix.

Figure 1 illustrates the maximum likelihood estimation concept. The measured response of the aircraft is compared with the estimated response. The difference between these responses is called the response error. The Newton-Balakrishnan[1,6,7] computational algorithm (formerly referred to as the modified Newton-Raphson algorithm) is used to find the derivative values that maximize the likelihood functional. Each iteration of this algorithm provides a new estimate of the unknown coefficients on the basis of the response error. The new estimates of the coefficients are then used to update the mathematical model of the aircraft. The updated mathematical model is used to provide a new estimated response and, therefore, a new response error. The updating of the mathematical model continues iteratively until a convergence criterion is satisfied. The estimates resulting from this procedure are the maximum likelihood estimates.

## Recent Maximum Likelihood Estimation Investigations

For the past 11 years analytical studies have been conducted at the authors' organization using the maximum likelihood estimation method to obtain estimates of coefficients from dynamic maneuvers. During these studies nearly 3000 flight maneuvers from 30 aircraft have been used for the extraction of stability and control derivatives. References 2 and 3 report some of the results obtained and the techniques developed to enhance the quality of the estimates. In addition to those previously reported, studies have been made on maneuvers performed with the Beech 99, Minisniffer, B-1, F-15, F-17, and oblique-wing[12] aircraft and the shuttle carrier aircraft with and without the shuttle vehicle.

The characteristics of some of these vehicles and the new flight regimes now being investigated have prompted the development of a general maximum likelihood estimation program called MMLE 3. The first version of the modified maximum likelihood estimation program, MMLE,[6] is still used for most of the routine extraction of stability and control derivatives, but MMLE 3 is used where more generality is required. MMLE 3 is a maximum likelihood estimation program capable of handling general bilinear dynamic equations of arbitrary order with or without state noise. It is not restricted to a particular set of dynamic equations or observations. The program has been used to analyze data obtained from the oblique-wing vehicle and from aircraft with structural/aerodynamic mode coupling. It has also been applied to maneuvers obtained in atmospheric turbulence.

The reliability and quality of stability and control derivative estimates can be increased by careful application of these programs. References 2 and 3 discuss many of the problems that can arise from careless application of the maximum likelihood estimation method. Additional considerations are discussed in the following sections.

## Cramer-Rao Bounds

To make effective use of the derivative estimates obtained from flight data, it is necessary to have some measure of the reliability of the estimates. If a large number of maneuvers are available, the amount of scatter of the estimates provides a reasonable indication of the reliability. When only a few maneuvers are available, other measures of reliability must be used. Even with many maneuvers, it would be useful to know if some of the estimates were more reliable than others; this information cannot be easily gleaned from the scatter. The Cramer-Rao bound[1,13] is the best of the known theoretical measures of the reliability of the estimates and the relative amount of information contained in a maneuver. This bound can be readily computed from the information available in maximum likelihood estimation programs, which has led to widespread use of the bound.

In spite of the strong theoretical rigor behind the Cramer-Rao bound, it would be wise to test it by evaluating its reasonability on typical aircraft data before placing too much dependence on it. A simple reasonability check can be made by comparing the Cramer-Rao bound with the amount of scatter of the estimates. Figure 2 illustrates this comparison for simulated data with artificial Gaussian white measurement noise. The scales of the figure are expanded to show the effect. The symbols indicate the maximum likelihood estimates of $C_{n_\beta}$ and $C_{l_\beta}$ based on the data from eighteen simulated maneuvers with measurement noise added. Derivatives and input signals were taken from the PA-30 flight data discussed in the following paragraph and used to create the simulated data. The magnitude of the simulated measurement noise was chosen to make the scatter of $C_{l_\beta}$ and $C_{n_\beta}$ typical of the scatter observed in flight data. The vertical bars show the magnitudes of the Cramer-Rao bounds. In theory, the magnitudes of the Cramer-Rao bounds should approximately equal the standard deviations of the estimates. This can be visually verified in Fig. 2.

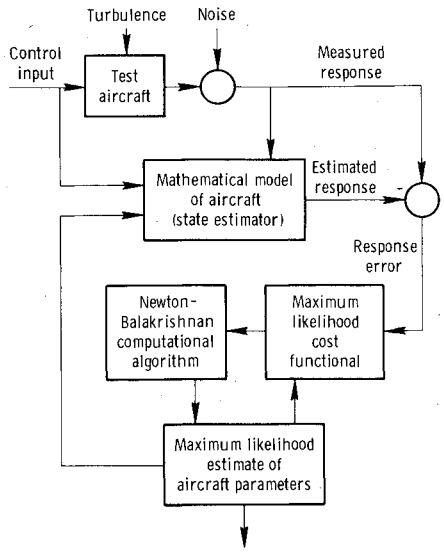


Fig. 1 Maximum likelihood estimation concept.

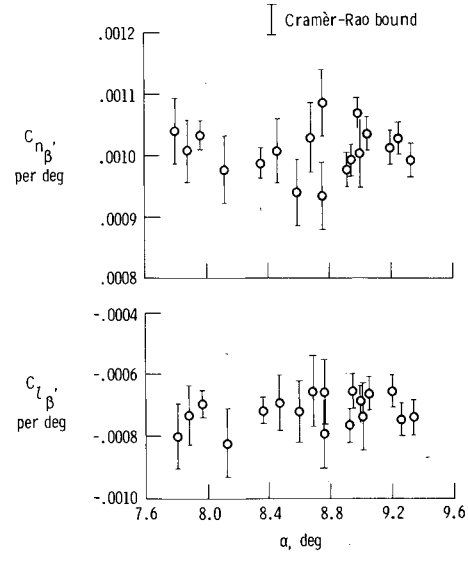


Fig. 2 Stability derivative estimates and Cramer-Rao bounds for computed data.

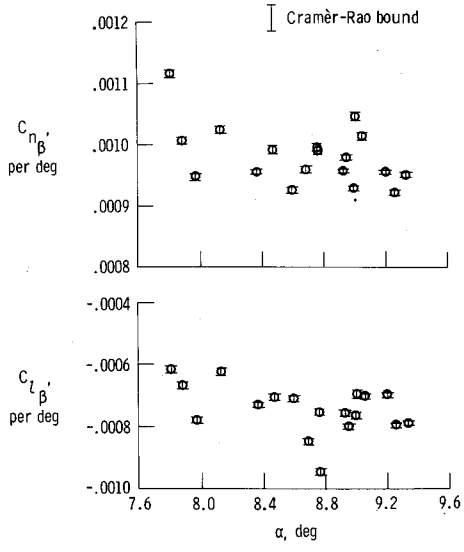


**Fig. 3 Stability derivative estimates and Cramer-Rao bounds for flight data.**

Although the Cramer-Rao bound checks out excellently on computed data, it has long been known that a large anomaly exists in results from flight data. Figure 3 shows a comparison of the same type as that shown in Fig. 2, except that the actual flight data from the PA-30 aircraft were used to obtain the derivative estimates and the Cramer-Rao bounds. These data were obtained at the same flight condition as was used for the previous simulated data. The data scatter in Fig. 3 is obviously far larger than predicted by the Cramer-Rao bounds. This phenomenon of larger scatter than predicted by the Cramer-Rao bound is common to all flight data. It has proven useful to multiply the Cramer-Rao bound by a factor of 5 to 10 to make it representative of the scatter observed in flight data.[3] This factor, however, was purely empirical and no rigorous theoretical explanation was available for why the disagreement existed and whether it could be properly accounted for by a constant factor. The necessity for this unexplained factor considerably weakened the confidence that could be placed in the Cramer-Rao bound.

Recent investigations have shown that the disagreement may be explained by carefully accounting for the spectral characteristics of the residual errors of flight data. Previous analysis has assumed that the measurement noise was band-limited white, with the band limit equal to the Nyquist frequency, $1/(2\Delta t)$ (typically 10-25 Hz). A band limit of approximately 1 Hz is more typical of that observed on actual data, but the Nyquist frequency was chosen as the assumed band limit because the frequency of the band limit did not seem important and because the assumption of the Nyquist frequency greatly simplified the analysis in the discrete time case (the noise samples at each point were then independent). However, if the primary analysis is done in continuous time and discretized for the actual computation only at the last step of analysis, it is equally easy to assume any band limit. In fact, the maximum likelihood estimation algorithm and the Cramer-Rao bound are both unaffected by the band limit in the continuous-time analysis, provided only that the noise band limit is well above the system bandwidth.

This result seems to verify the earlier assumption that the bandwidth is unimportant to the analysis. However, the bandwidth is also used explicitly (in the continuous-time case) or implicitly (in the discrete-time case) to determine the weighting matrix, $(GG^*)^{-1}$, from real data. The usual procedure to compute $GG^*$ is to compute the total power of the residual error and divide by the Nyquist frequency; in the discrete-time case the total power itself is used and the division by the Nyquist frequency is done implicitly in the algorithm.

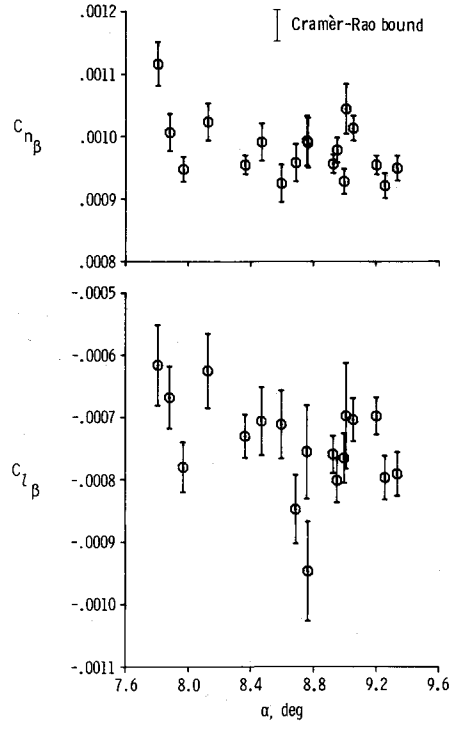


**Fig. 4 Stability derivative estimates and Cramer-Rao bounds for flight data obtained by modifying assumed spectral densities.**

The source of the problem can be easily seen. If the band limit is lower than the Nyquist frequency, the usual computation of the spectral density will be incorrect; the total power should properly be divided by the actual band limit instead of the Nyquist frequency. Since actual data are not strictly band limited but decrease in power over a finite frequency range, some error is inherent in selecting any single frequency as the band limit. This error, however, would be of an acceptable magnitude, unlike the factor-of-25 error between a realistic 1 Hz band limit and the 25 Hz Nyquist frequency of data obtained at 50 samples per second. Since the Cramer-Rao bound is given by the square root of

$$\text{Variance}\,(\xi) \geq \left[\int_0^T \nabla_\xi (\hat{z}_\xi - z)^* (GG^*)^{-1} \nabla_\xi (\hat{z}_\xi - z)\,dt\right]^{-1}$$

errors in the determination of the spectral density $G$ will directly influence the bound.

The flight data from Fig. 3 can be used to illustrate these principles. An average band limit of approximately 1 Hz was observed from the power spectral densities of the residual measurement errors. This increased the estimate of $G$ by a factor of 5 over that obtained when the 25 Hz Nyquist frequency was assumed to be the band limit. Figure 4 shows the resulting Cramer-Rao bounds, which are five times larger than those in Fig. 3. The agreement between the scatter and the Cramer-Rao bound is much better in Fig. 4.

Naturally, the same band limit does not have to be used for all the signals, in which case the change in the Cramer-Rao bound cannot be expressed as a simple factor, but the bound can still be computed simply by using the correct $G$ matrix. Other acceptable methods of estimating $G$ are available, including direct examination of the magnitude of the power spectral density of the residual error. This study has shown, however, that the method used in current programs is significantly in error and that a constant factor is a reasonable first-order approximation of this error. These results are consistent with the good agreement already observed on simulated data because the additive noise used with the simulated data studies was band limited at the Nyquist frequency. Recent simulated data studies have succeeded in

reproducing the disagreement observed in flight data by using simulated noise with lower bandwidths. This lends support to the interpretation of the Cramer-Rao bound presented here.

## Aircraft Scale Effects

One way to assess the quality of flight estimates is to compare these estimates with predictions from other sources. When making this comparison, great care must be taken to assess any possible sources of error that may contaminate the estimates or predictions. Errors may enter into the flight-determined maximum likelihood estimates from many sources, some of which are discussed elsewhere in this paper. Other sources of error are discussed in Ref. 3. Sometimes after all apparent sources of error have been investigated, differences between the estimates from different sources still exist. This has been observed when comparing wind tunnel estimates with flight-determined estimates. These differences are frequently attributed to either scale effects or the differences in aerodynamic flow between the static wind tunnel tests and the dynamic flight maneuvers. It is, therefore, of interest to compare flight-determined estimates from the same configuration for two scales.

The F-15 airplane (described in Ref. 14) and the 3/8-scale model F-15 remotely piloted research vehicle (RPRV)[15] are of the same configuration. Other than scale, the primary difference between the two vehicles is that the F-15 RPRV is unpowered with blocked inlets and the F-15 airplane is powered. An assessment of this difference can be made by performing maneuvers at different engine mass flow rates with the F-15 airplane.

Stability and control maneuvers were performed on the F-15 airplane and the F-15 RPRV. The maneuvers on the F-15 airplane were performed at three engine mass flow rates to assess the effect of the propulsion system on the stability and control derivatives. A complete set of stability and control derivatives was obtained for both vehicles using the maximum likelihood estimation method. These derivatives were obtained on both vehicles over an angle-of-attack range of approximately $-15$ to 20 deg. The propulsion system appeared to have little effect on the derivatives. In general, very good agreement was found between the estimates from the two vehicles.

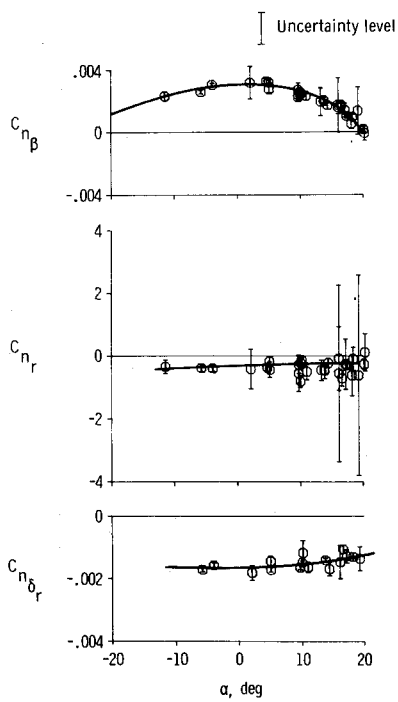


**Fig. 5 Selected low-speed stability and control derivatives as functions of angle of attack obtained from 3/8-scale F-15 RPRV.**

Figure 5 shows the maximum likelihood estimates of $C_{n_\beta}$, $C_{n_r}$, and $C_{n_{\delta_r}}$ from the F-15 RPRV. The vertical bars represent the uncertainty levels.[3] The fairing of the data was determined by considering the estimates with the smaller uncertainty levels to be more reliable. Figure 6 presents estimates from the F-15 airplane of the same derivatives in the same format. The various symbols represent various mass flow rates. The fairing from Fig. 5 is repeated in Fig. 6. The agreement between the two vehicles is good for $C_{n_\beta}$ and $C_{n_r}$. The trend for $C_{n_{\delta_r}}$ is the same for both vehicles, but the F-15 airplane indicates more rudder control effectiveness. There is no trend in $C_{n_{\delta_r}}$ for the F-15 airplane to indicate that an extrapolation of the mass flow rates would account for this difference. Since $C_{n_\beta}$ and $C_{n_r}$ for both vehicles are in good agreement, it is unlikely that an error in the moment of inertia in one of the vehicles would account for the difference. Therefore, the difference in $C_{n_{\delta_r}}$ between these vehicles may be attributable to scale effects.

## A Multiple Minima Problem

All aircraft have observable structural modes. These modes usually cause no difficulty in estimating stability and control derivatives because the structural frequencies are higher than the aerodynamic frequencies. In general, if the structural frequencies are higher than the highest aerodynamic frequency by more than a factor of 5 to 10, they can be neglected, unless their amplitude is so large as to mask measurements desired for the aerodynamic analysis. However, if one or more structural modes are affecting the aerodynamic modes, as is common in large aircraft, these structural modes must be included in the mathematical model being analyzed.

It is useful to assess the time domain analysis of the structural modes independent of any interaction. This can be done where a structural mode is observed and no significant coupling is detected.

Figure 7 shows a structural mode observed at 200 samples per second on the lateral acceleration of an aircraft where little effect was observed for structural/aerodynamic coupling. The frequency of the mode is high enough so that the mode does not interact with the aerodynamic modes. Therefore, the stability and control derivatives were obtained separately and held constant for the succeeding analysis. The analysis consisted of using the maximum likelihood estimation program MMLE 3 with a sixth-order model that included the lateral-directional aerodynamic modes plus one structural mode. The dynamic pressure and the velocity were

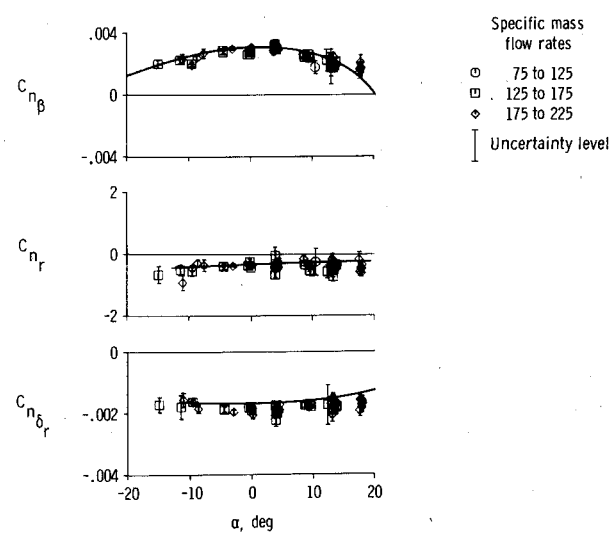


**Fig. 6 Selected low-speed stability and control derivatives as functions of angle of attack obtained from F-15 airplane at three engine mass flow rates.**

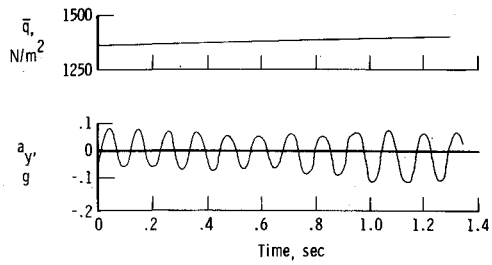


**Fig. 7 Structural mode oscillation observed on the lateral acceleration.**

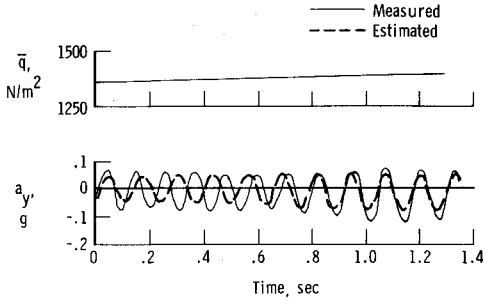


**Fig. 8 Fit of measured and computed lateral acceleration obtained when maximum likelihood estimator converged to local minimum.**

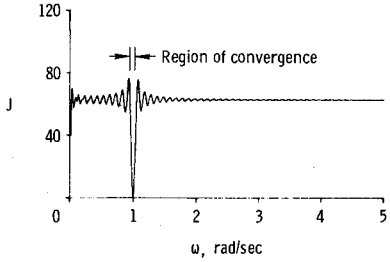


**Fig. 9 Cost functional for ten cycles of data as function of frequency showing close proximity of local minima to global minimum.**

allowed to vary in the analysis. The structural mode frequency and damping were both estimated as linear functions of dynamic pressure. The initial conditions were also estimated. A structural mode frequency of 7.84 Hz was chosen to start the estimation process. The comparison between the original data and the fit obtained with the maximum likelihood estimation method is shown in Fig. 8. The two time histories are in good agreement at the beginning and the end of the maneuver, but they are 180 deg out of phase at a time of approximately 0.3 s. The fit shown in Fig. 8 suggests that the maximum likelihood estimator has reached a local minimum but not the global minimum. Multiple minima are not normally a problem when obtaining the stability and control derivatives with the maximum likelihood estimation method. They can be a problem, however, if a technique is used that incorporates the extended Kalman filter. Multiple minima have been observed when the short-period and phugoid modes are analyzed simultaneously with the maximum likelihood estimation technique. This problem is caused by the long record length required to identify the coefficients of the phugoid mode. The long record length dictates that many cycles of the short-period mode occur and, if the short-period coefficients are not started very close to the correct answer, multiple minima occur. Experience has shown that it is best to first determine the short-period characteristics and then hold those constant while the phugoid characteristics are determined. The problem observed in Fig. 8 is similar to the short-period analysis just discussed in that many cycles of the structural mode are observed.

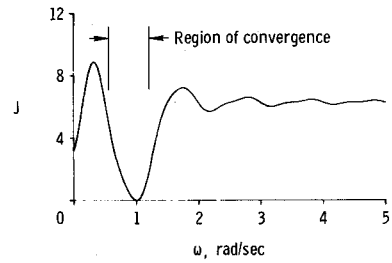


**Fig. 10 Cost functional of one cycle of data as function of frequency showing wide region of convergence for global minimum.**

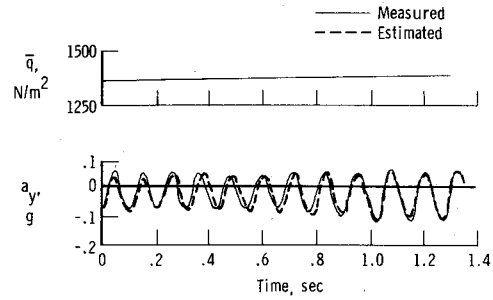


**Fig. 11 Acceptable fit of measured and computed lateral acceleration.**

The reason for the multiple minima is demonstrated by the following simple scalar example.

Let the noiseless measured response be

$$y(t) = \sin \omega_0 t$$

and the estimated response be

$$y_\xi = \sin(\omega t)$$

where $\omega$ is the only unknown coefficient. Then, by Eq. (1), the cost functional becomes

$$J(\omega,T) = \int_0^T [\sin(\omega_0 t) - \sin(\omega t)]^2 dt$$

$$= T - \frac{1}{4\omega_0}\sin(2\omega_0 T) - \frac{1}{4\omega}\sin(2\omega T)$$

$$- \frac{2\omega}{\omega^2 - \omega_0^2}\left[\frac{\omega_0}{\omega}\sin(\omega T)\cos(\omega_0 T) - \cos(\omega T)\sin(\omega_0 T)\right]$$

If $T$ is chosen to represent 10 cycles as shown in Fig. 8, then for an $\omega_0$ of 1 rad/s, $T$ equals $20\pi$.

The cost functional $J(\omega,20\pi)$ is shown as a function of $\omega$ in Fig. 9. The global minimum is at an $\omega$ of 1 rad/s as it should be, but there are many local minima at increments of approximately 0.05 rad/s. If a value of less than 0.97 or greater than 1.03 were chosen for a starting estimate of $\omega$, the algorithm would converge to a local minimum. If a value of between 0.98 and 1.02 were chosen, it would converge to the global minimum. Therefore, for this example where 10 cycles were observed, the starting value of $\omega$ must be less than 3% from the correct answer to converge to the global minimum.

If $T$ is chosen to represent only one cycle and $\omega_0$ remains equal to 1 rad/s, then $T$ equals $2\pi$.

The cost functional $J(\omega,2\pi)$ is presented as a function of $\omega$ in Fig. 10. The global minimum is correctly at an $\omega$ of 1 rad/s, but now the algorithm converges to the global minimum if $\omega$ is started within approximately 25% of the correct value.

Knowing the sensitivity of the algorithm when a record with many lightly damped cycles is being analyzed, the data of Fig.

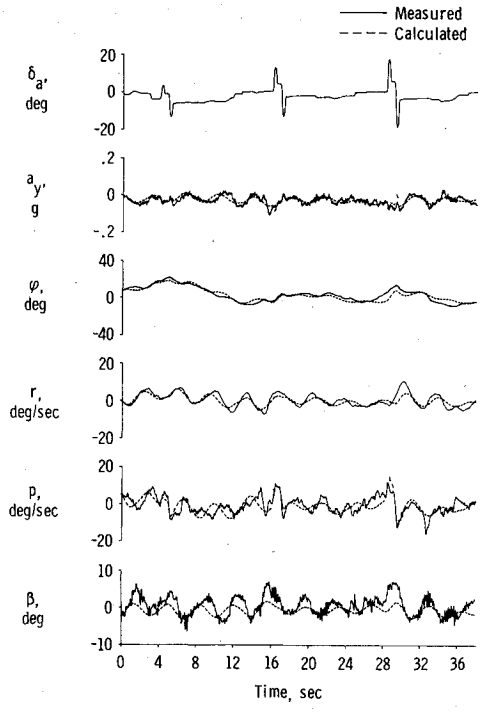


**Fig. 12 Fit of flight data obtained in turbulence and computed data obtained from maximum likelihood estimator that does not account for turbulence.**

7 can be reanalyzed starting closer to the observed frequency. Starting the maximum likelihood estimation method with an $\omega$ of 9.0 results in the fit shown in Fig. 11. This is an acceptable fit of the data.

Based on the preceding results, if data are to be analyzed where many cycles of a structural mode are present, the structural mode frequency $\omega$ must be closely approximated before starting the estimation process.

## Atmospheric Turbulence Analysis

Aircraft cannot always avoid flying in atmospheric turbulence, so it is desirable to be able to obtain stability and control derivatives in the presence of turbulence. In addition, it can also be important to obtain an estimate of the turbulence time history. This is particularly of interest in the implementation of turbulence suppression systems.

It has been demonstrated for many years that the stability and control derivatives can be adequately determined with maximum likelihood estimators for maneuvers performed in smooth air. If these techniques, which do not account for turbulence, are applied to data obtained in turbulence, not only are the resulting fits of the time histories unsatisfactory but the estimated coefficients are unacceptable.[8-10] The technique described in Refs. 7-10 can account for the effect of turbulence. With this technique, maximum likelihood estimates of the stability and control derivatives as well as estimates of the turbulence time histories are obtained by minimizing the cost functional given by Eq. (2). Results of the application of the technique to longitudinal maneuvers obtained in turbulence have been presented previously.[8-10]

The lateral-directional equations can be modified in a manner similar to that used to modify the longitudinal equations in Refs. 8 and 10. The turbulence model is the Dryden expression, which is described in Ref. 16. With these modifications, MMLE 3 can be used to obtain the maximum likelihood estimates.

Thirty-eight seconds of data from the PA-30 aircraft flying in turbulence were analyzed at 50 samples per second. The best fit that could be obtained with the maximum likelihood estimation method that does not account for turbulence is shown in Fig. 12. The fit is unacceptable and resulted in poor estimates of the stability and control derivatives. Figure 13 shows the fit obtained with the maximum likelihood estimation technique that accounts for turbulence. The fit is virtually perfect and the maneuver provided acceptable estimated stability and control derivatives. The residual error in angle of sideslip is due to a structural vibration affecting the sensor. It is also of interest to compare the power spectra of the estimated turbulence time histories. The power spectrum of the turbulence component affecting angle of sideslip, $\hat{\beta}_g$, is shown in Fig. 14. Figure 15 presents the power spectrum of the turbulence component affecting roll rate, $\hat{p}_g$. The

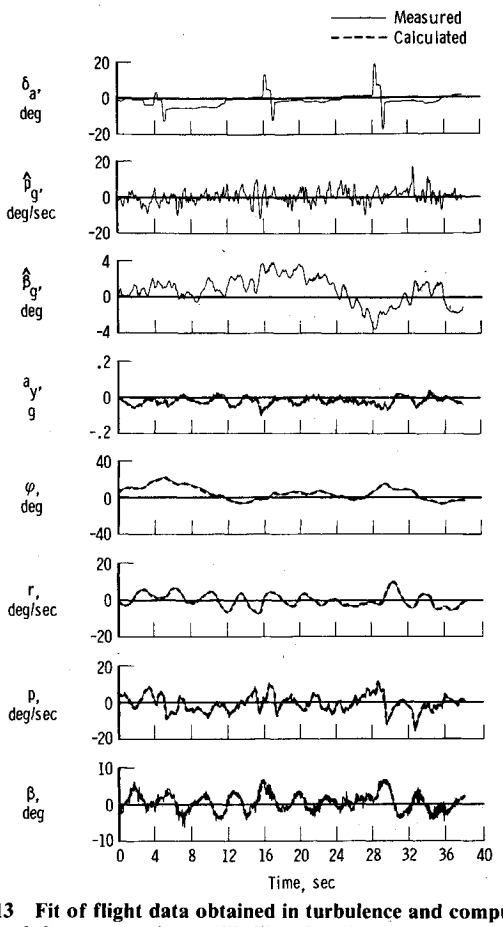


**Fig. 13 Fit of flight data obtained in turbulence and computed data obtained from a maximum likelihood estimator that accounts for turbulence.**

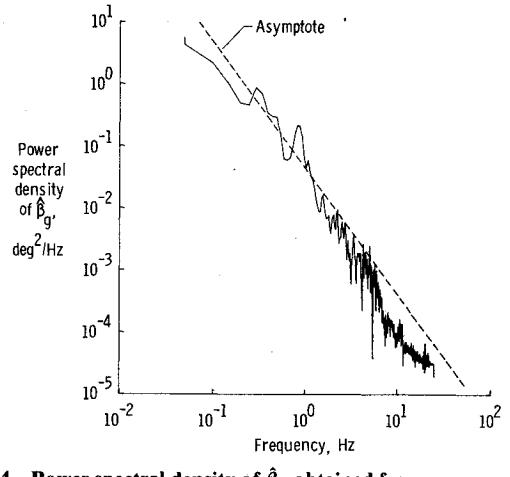


**Fig. 14 Power spectral density of $\hat{\beta}_g$ obtained from maneuver shown in Fig. 13.**

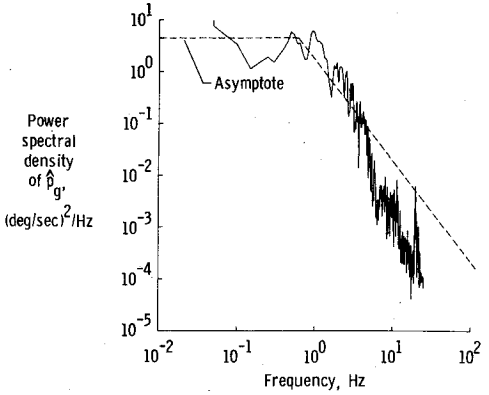


**Fig. 15 Power spectral density of $\hat{p}_g$ obtained from maneuver shown in Fig. 13.**

slopes of the asymptotes shown in Figs. 14 and 15 are those defined by the Dryden expression. Good agreement is shown between the power spectra and the asymptotes for $\hat{\beta}_g$ and $p_g$.

## Conclusions

This paper discussed the application of a maximum likelihood estimation method to flight test data. The following important conclusions were made:

1) The Cramer-Rao bound is representative of the scatter observed in flight data if the spectral densities of the residual measurement errors are properly accounted for.

2) Although most of the derivatives obtained from flight for two similar vehicles of different scales were in good agreement, the coefficient of yaw due to rudder deflection $C_{n_{\delta_r}}$ was higher for the larger scale airplane.

3) If many cycles of lightly damped data are obtained, the maximum likelihood estimation method must start very close to the correct answer to assure that the global minimum is attained.

4) The maximum likelihood estimation method that accounts for turbulence provided a good fit with the lateral-directional measured data, acceptable estimates of the stability and control derivatives, and estimated turbulence in good agreement with the theoretical Dryden expression.

## References

[1] Iliff, K.W. and Taylor, L.W., Jr., "Determination of Stability Derivatives From Flight Data Using a Newton-Raphson Minimization Technique," NASA TN D-6579, 1972.

[2] Iliff, K.W. and Maine, R.E., "Practical Aspects of Using a Maximum Likelihood Estimator," *Methods for Aircraft State and Parameter Identification*, AGARD-CP-172, May 1975, pp. 16-1-16-15.

[3] Iliff, K.W. and Maine, R.E., "Practical Aspects of Using a Maximum Likelihood Estimation Method to Extract Stability and Control Derivatives From Flight Data," NASA TN D-8209, 1976.

[4] Iliff, K.W. and Maine, R.E., "Further Observations on Maximum Likelihood Estimates of Stability and Control Characteristics Obtained from Flight Data," *Proceedings of AIAA Atmospheric Flight Mechanics Conference,* Hollywood, Fla., 1977, pp. 100-112.

[5] Goodwin, G.C. and Payne, R.L., *Dynamic System Identification: Experiment Design and Data Analysis,* Academic Press, New York, 1977.

[6] Maine, R.E. and Iliff, K.W., "A FORTRAN Program for Determining Aircraft Stability and Control Derivatives From Flight Data," NASA TN D-7831, 1975.

[7] Balakrishnan, A.V., "Stochastic Differential Systems I. Filtering and Control – A Function Space Approach," *Lecture Notes in Economics and Mathematical Systems,* Vol. 84, edited by M. Beckmann, G. Goos, and H.P. Kunzi, Springer-Verlag, Berlin, 1973.

[8] Iliff, K.W., "Identification and Stochastic Control With Application to Flight Control in Turbulence," School of Engineering and Applied Science, University of Calif., Los Angeles, Calif., UCLA-ENG-7340, May 1973.

[9] Schulz, G., "Influence of Gust Modeling On the Identification of the Derivatives of the Longitudinal Motion of an Aircraft," Royal Aircraft Establishment Library Translation 1944, 1977.

[10] Yazawa, K., "Identification of Aircraft Stability and Control Derivatives in the Presence of Turbulence," AIAA Paper 77-1134, AIAA Atmospheric Flight Mechanics Conference, Hollywood, Fla., 1977.

[11] Powell, J.D. and Tyler, J.S., "Application of the Kalman Filter to VTOL Parameter Identification," JACC Conference, June 1970.

[12] Maine, R.E., "Maximum Likelihood Estimation of Aerodynamic Derivatives for an Oblique Wing Aircraft From Flight Data," AIAA Paper 77-1135, AIAA Atmospheric Flight Mechanics Conference, Hollywood, Fla., Aug. 1977.

[13] Klein, V., "On the Adequate Model For Aircraft Parameter Estimation," Cranfield Report Aero No. 28, 1975.

[14] Wilson, D.B. and Winters, C.P., "F-15A Approach-to-Stall/Stall/Post-Stall Evaluation," Air Force Flight Test Center, Edwards Air Force Base, AFFTC-TR-75-32, Jan. 1976.

[15] Iliff, K.W., Maine, R.E., and Shafer, M.F. "Subsonic Stability and Control Derivatives for an Unpowered, Remotely Piloted 3/8-Scale F-15 Airplane Model Obtained From Flight Test," NASA TN D-8136, 1976.

[16] Chalk, C.R., Neal, T.P., Harris, T.M., Pritchard, F.E., and Woodcock, R.J., "Background Information and User Guide for MIL-F-8785B (ASG), Military Specification-Flying Qualities of Piloted Airplanes," Air Force Flight Dynamics Lab., Wright-Patterson Air Force Base, AFFDL-TR-69-72, Aug. 1969.